Fish and Shellfish Immunology 92 (2019) 1–10

Contents lists available at ScienceDirect

Fish and Shellfish Immunology

journal homepage: www.elsevier.com/locate/fsi

Full length article

Identification and characterization of a symbiotic agglutination-related C-type lectin from the hydrothermal vent shrimp *Rimicaris exoculata*

Xiao-Li Liu[a], Sen Ye[a], Cai-Yuan Cheng[a], Hua-Wei Li[a], Bo Lu[b], Wei-Jun Yang[a], Jin-Shu Yang[a,*]

[a] College of Life Sciences, Zhejiang University, Hangzhou, Zhejiang, 310058, PR China
[b] Key Laboratory of Marine Ecosystem and Biogeochemistry, State Oceanic Administration, Second Institute of Oceanography, Ministry of Natural Resources, Hangzhou, Zhejiang, 310012, PR China

ARTICLE INFO

Keywords:
C-type lectin
Hydrothermal vent
Rimicaris exoculata
Symbiosis
Pattern recognition receptor
Microbial recognition

ABSTRACT

Rimicaris exoculata (Decapoda: Bresiliidae) is one of the dominant species of hydrothermal vent communities, which inside its gill chamber harbors ectosymbioses with taxonomic invariability while compositional flexibility. Several studies have revealed that the establishment of symbiosis can be initiated and selected by innate immunity-related pattern recognition receptors (PRRs), such as C-type lectins (CTLs). In this research, a CTL was identified in *R. exoculata* (termed RCTL), which showed high expression at both mRNA and protein levels in the scaphognathite, an organ where the ectosymbionts are attached outside its setae. Linear correlationships were observed between the relative quantities of two major symbionts and the expression of RCTL based on analyzing different shrimp individuals. The recombinant protein of RCTL could recognize and agglutinate the cultivable γ-proteobacterium of *Escherichia coli* in a Ca^{2+}-dependent manner, obeying a dose-dependent and time-cumulative pattern. Unlike conventional crustacean CTLs, the involvement of RCTL could not affect the bacterial growth, which is a key issue for the successful establishment of symbiosis. These results implied that RCTL might play a critical role in symbiotic recognition and attachment to *R. exoculata*. It also provides insights to understand how *R. exoculata* adapted to such a chemosynthesis-based environment.

1. Introduction

The hydrothermal vent is a special ecosystem in the deep ocean usually found along the mid-ocean ridges and back-arc basins such as the Mid-Atlantic Ridge (MAR), East Pacific Rise (EPR) and Central Indian Ridge (CIR). Unlike terrestrial or shallow watery environments where life has traditionally been seen as driven by energy from the sun, deep-sea hydrothermal-vent organisms have no access to sunlight. Instead they have to depend on materials from ambient dusty chemical deposits and hydrothermal fluid. As primary producers, large populations of chemoautotrophic bacteria can oxidize reduced chemicals like H_2S and methane to produce energy to drive carbon-fixation processes [1]. For other larger species living in the interfacial zone where hydrothermal fluid mixes turbulently with bottom seawater, these autotrophic bacteria play an indispensable role either as the food source or as the detoxification helper [3,8]. This long-term interdependence prompted different types of symbioses (endo- or ecto-symbiosis) occurring in vent animals such as tubeworms, mussels, and crustaceans (such as bresiliid shrimps, galatheid and bythograeid crabs).

The bresiliid shrimp *Rimicaris exoculata* [2], one of the dominant species at most hydrothermal vents along MAR [3], harbors a rich community of external symbiotic bacteria in its modified mouthparts, mainly on setae of scaphognathites and exopodites specialized from the 2nd maxillae and the 1st maxillipeds, respectively [4,5]. Early results from 16S rRNA genotyping and fluorescence *in situ* hybridization (FISH) revealed that, wherever collected from different sites of MAR, a limited group of phylotypes belonging to proteobacteria dominate the shrimp ectosymbionts, with other types of bacteria only accounting for a smaller portion [4,6,7]. In general, most deep-sea endemic animals renew their symbionts by horizontal acquisition once per each host generation [9]. In *R. exoculata*, the situation becomes more frequent and complicated: the symbiotic bacteria attached to its chitinous exoskeleton would be eliminated and regained after each molt, a characteristic cyclic process for all arthropods [10]. How does the host distinguish candidate symbionts from the pool of diverse free-living bacteria in the surroundings? Why could these specific bacteria regularly form long-term symbiotic relationships with their host? An ideal explanation is specific and stable recognition between the host and mutualistic bacteria. However, until now we know little about the underlying mechanism to establish this kind of recognition relationships

* Corresponding author.
E-mail address: yjsdos@zju.edu.cn (J.-S. Yang).

https://doi.org/10.1016/j.fsi.2019.05.057
Received 29 January 2019; Received in revised form 16 May 2019; Accepted 25 May 2019
Available online 26 May 2019

Table 1
Primers and oligonucleotide probes used in this study.

Primer	Length (nt)	Direction[a]	Sequence (5′–3′)[b]
RCTL-F	19	F	GGAAGGGGTGGAAGGGAGG
RCTL-R	30	R	AAGCAATTAGTAATGTCTTGAAAAGCAAAT
qRCTL-F	26	F	ATATCGGCAGTATGAGTTGGGGAGA
qRCTL-R	26	R	GTTAGTTCAAATTGCTGGAGGTGT
18SF	27	F	GCTGTGGATTGTAGGCCATGCGCCTAC
18SR	27	R	GGCTGCTGGCACCAGACTTGCCCTCCAA
*Bam*HI-RCTL-F	26	F	CG**GGATCC**TTAGAGTGTGACAGTGTC
*Xho*I-RCTL-R	29	R	CCG**CTCGAG**TTATCTGAAAATAGTTTGTTGTT
Q16s-gamaF	24	F	GCAGAGATGCGGGAGTGTCCTTCG
Q16s-gamaR	26	R	GTCCCCGCCTTCCTCCAGTTTGTTCA
Q16s-deltF	24	F	AGTGCCTCATTAGAGGAACCTGGTGA
Q16s-deltR	26	R	AGTCCCTCTGGAGTGCCCAACTGAAT
Q16s-epsyF	27	F	CAACCCTCGTGTTTAGTGCTAACAGTT
Q16s-epsyR	25	R	CGGTATTGCGTCTCACTTGTCCTAA
EPSY105	18	–	TATACATTACTCACCCGT
GAM615	18	–	CAGATGCAGTTCCCAGGT
DELT241	18	–	AACTAGCTAATGGTACGC

[a] F, forward; R, reverse.
[b] Recognition sequences of restriction endonucleases are shown in bold.

in *R. exoculata*.

Interaction with symbiotic microbes is commonly viewed in the same way as the immunity against pathogens. Like all other invertebrates the shrimp lacks an advanced antibody-based adaptive immunity like in vertebrates and only possesses an innate immune system. Invertebrates respond against microorganisms in three main ways: the recognition by pattern recognition receptors (PRRs), the cellular immunity in the form of the phagocyte response, and the humoral components comprised of acellular and biochemical factors [11]. The most important step of these processes is the initial recognition of the foreign objects that relies on PRRs' binding microbe-associated molecular patterns (MAMPs) present on the microbial surface [12]. Both symbiotic and pathogenic microbes share the common mechanisms directing recognizing interactions. For instance, a mannose-binding lectin (millectin) isolated from the coral *Acropora millepora* could bind both pathogens and symbionts [13]. In human, both of symbiotic *Bacteroides thetaiotaomicron* and pathogenic *Porphyromonas gingivalis* can induce the Toll-like receptor 4 (TLR4) pathway of immune response [14]. However, unlike in pathogenic elimination, in the case of symbiosis, the recognition events would not result in the subsequent destruction of invading microbes but in the production of adhesion mediators, or formation of special organs to hold these mutualistic neighbors, like the light organ in the squid *Euprymna scolopes* [15] and the trophosome in the tubeworm *Riftia pachyptila* [16].

Lectin is one group of important PRRs mediating recognition between hosts and symbionts. Besides the aforementioned coral millectin, symbiosis-related lectins have been already identified in legume/nitrogen-fixing bacteria mutualisms [17], as well as symbioses between bacteria and sponge [18] or lichen [19]. In invertebrates, all symbiotic lectins identified to date belong to the subgroup of C-type lectins (CTLs). For examples, in the symbiosis between the marine nematode *Laxus oneistus* and a sulfur-oxidizing bacterium there identified host-expressed CTLs (Mermaids) that could mediate symbiotic adhesion to the worm cuticle [20]. Similarly, in the clam *Codakia orbicularis*, a mannose-binding CTL (codakine) is involved in the recognition of its sulfur-oxidizing symbionts [21]. All CTLs share at least one common carbohydrate recognition domain (CRD) for binding carbohydrates usually in a Ca^{2+}-dependent manner [22]. By binding the carbohydrate components of MAMPs like LPS and peptidoglycan, CTLs can specifically interact with and agglutinate exogenous microbes. Most research has been focusing on the process of pathogen infection, and how they induce immune responses. However, little study was concerned with the subsequent process happening in CTL-directing symbioses.

In this research, a C-type lectin (RCTL) was identified with high expression at both mRNA and protein levels in the *R. exoculata* scaphognathite where vast symbionts are attached to the outside surfaces of its setae. This relationship was confirmed by the correlation analysis between the relative quantities of different symbionts and the expression of RCTL in shrimp individuals. The recombinant protein of RCTL could recognize and agglutinate the γ-proteobacterium of *Escherichia coli* in a Ca^{2+}-dependent manner. The agglutination of RCTL with bacteria appeared time-cumulative and dose-dependent, without obvious effect on bacterial growth. These results suggest that RCTL plays a critical role in symbiont recognition and attachment in *R. exoculata*. This is the first immune-related molecule that can mediate symbiosis in crustaceans. Our study will help to understand how the crustacean established a symbiotic relationship with selected mutualistic bacteria so as to adapt to chemosynthesis-based environments like hydrothermal vents.

2. Materials and methods

2.1. Sample collection

The hydrothermal-vent shrimps *Rimicaris exoculata* were collected at the south Mid-Atlantic Ridge (15°9′ S, 13°21′ W, 2741 m) on Jun. 4th, 2011, during the cruise DY115-22V-SMAR-S024-TVG05. The specimens were immediately stored in liquid N_2 and then transferred to −80 °C until used.

2.2. Molecular cloning and sequence analysis of RCTL

A full-length cDNA sequence of the C-type lectin (RCTL) was obtained from a scaphognathite transcriptome library of *R. exoculata* (unpublished data). The nucleotide sequence was confirmed by specific primers designed based on this pyrosequenced transcript (Table 1). Total RNA was isolated from scaphognathites using TRIzol reagent (Invitrogen, USA). The cDNA synthesis was carried out by M-MLV reverse transcriptase (TaKaRa, Japan) in a reaction volume of 20 μL containing 2 μg of total RNA.

Nucleotide and amino acid sequences were analyzed using the BLAST program (http://www.ncbi.nlm.nih.gov/blast). The signal peptide in this sequence was predicted by the SignalP 4.1 software online (http://www.cbs.dtu.dk/services/SignalP/). A multiple sequence alignment of RCTL with other crustacean CTLs containing an LDLa domain was calculated by MEGA7 [23]. Amino acid sequences of C-type lectins from other non-vent crustaceans based on the BLAST result against the nr database were used for phylogenetic analysis. An

unrooted topology was generated by using the neighbor-joining (NJ) method implemented in MEGA7. Branch supports were calculated after 1000 bootstrap replicates. Homology modeling was performed on SwissModel (http://www.swissmodel.expasy.org/), and the protein visualization was made by Pymol [24]. The nucleotide sequence of RCTL was submitted to GenBank (https://www.ncbi.nlm.nih.gov/genbank/) under the accession number MK443495.

2.3. Gene expression and symbiont quantity by real-time PCR

Total RNA and genomic DNA of both host and symbiont were extracted from gills, hepatopancreas, muscle and scaphognathites of *R. exoculata* by using TRIzol reagent (Invitrogen, USA) as the manufacturer's instructions. The cDNA was synthesized as the method described above. The relative expression of RCTL was estimated by real-time PCR amplification using RCTL-specific primers (Table 1). The relative quantities of symbionts were estimated by amplification using genomic DNA as template and each type of symbiont was quantified by its specific 16S primers. The host 18S RNA gene served as an internal PCR control (Table 1). All experiments were carried out on the Bio-Rad MiniOpticon real-time PCR system using SYBR Premix Ex Taq (TaKaRa, Japan). Each reaction contains 1 μL template, 6.25 μL SYBR Premix Ex Taq, 4.75 μL ddH_2O and 0.25 μL each specific primer in a final volume of 12.5 μL. The data was analyzed using MxPro qPCR software (Stratagene, USA). Further quantitative analysis was performed using the $2^{(-\Delta\Delta Ct)}$ method [25].

2.4. Western blotting

The amino acid sequence of the deduced RCTL protein was analyzed and the best epitope (CIDVSNLNKSNQLA) was selected to prepare an antibody. The *anti*-RCTL antibody was raised in rabbit against this synthetic polypeptide (HuaAn, China). Protein was extracted with TRIzol reagent (Invitrogen, USA) as the manufacturer's instructions, dissolved in 2% SDS with 5 × Dual Color Protein Loading Buffer (Fude, China) and boiled for 10 min. After centrifugation at room temperature for 10 min, samples were separated on 10% SDS-PAGE gels and transferred to PVDF membranes (Millipore, USA). The membranes were incubated with primary antibodies (*anti*-RCTL antibody 1:2000; *anti*-β-actin antibody 1:5000) overnight at 4 °C. The secondary antibody was produced in goat to specifically recognize rabbit/mouse IgG (H + L) (Roche, Switzerland). Detection was performed using the BM Chemiluminescence Western Blotting Kit (Roche, Switzerland).

2.5. Expression and purification of the recombinant RCTL (rRCTL)

For the construction of the recombinant plasmid, the ORF of the RCTL mRNA was amplified using the primers *Bam*HI-RCTL-F and *Xho*I-RCTL-R (Table 1), dual-digested and ligated with pGEX-6p-2. After verification by sequencing, the constructed plasmid was purified with Plasmid Mini Kit I (Omega, China) and transformed into the *Escherichia coli* strain BL21. The bacterium including the expression plasmid was cultured in LB medium supplemented with ampicillin (50 μg/mL) at 37 °C until OD_{600} reached 0.6. A final concentration of 0.8 mM IPTG was added to induce the expression of the target protein. The culture was incubated at 18 °C for 16 h and cells were harvested by centrifugation at 6300 *g* for 10 min. Cell pellets were resuspended in PBS (containing 1% Triton X-100) and lysed by sonication (3s/3s, 70%) for 10 min in an ice bath. The GST-tagged protein in the supernatant was purified by Glutathione Sepharose 4B (GE Healthcare, USA) following the standard steps under non-denaturing conditions. Finally, the RCTL fusion protein was eluted in an elution buffer (10 mM glutathione, 50 mM Tris-HCl, pH 8.0). Protein concentration was determined using the BCA Protein Assay Kit (Sangon, China) after dialysis to remove glutathione. All components were analyzed by 10% SDS-PAGE.

2.6. Immunofluorescent assay

Scaphognathites were dissected from *R. exoculata* and transferred into 4% (w/v) paraformaldehyde immediately. After 14 h, the tissue was washed with PBS three times and then embedded in paraffin (Leica, USA). The embedded samples were cut into 5-μm-thick sections with a microtome (Leica EM UC6, USA). After dewaxing rehydrated, sections were boiled in antigen retrieval solution (0.01 M sodium citrate buffer, pH 6.0) for 15 min and then naturally cooled for 4 h to complete antigen retrieval. The slides were washed in PBS and blocked in antibody dilution buffer (PBS, 0.1% Triton X-100, 1% BSA) for 1 h followed by incubation with *anti*-RCTL antibody (1:200) overnight at 4 °C. After washed with PBS, the slides were incubated with the secondary Alexa Fluor 594-conjugated antibody in dark for 2 h at room temperature. The slides were examined with a laser scanning confocal microscope (Zeiss LSM710 NLO, Germany).

For immunofluorescence of the rRCTL-bacteria reaction, bacterial cultures were grown in LB medium until OD_{600} reached 0.6. Approximately 10 μL cultured bacteria were resuspended in 40 μL buffer A (50 mM Tris-HCl, 100 mM NaCl, 10 mM $CaCl_2$, pH 7.5) containing 4 μg rRCTL or GST protein incubated for 1 h at room temperature. The mixture was dropped onto the adhesive slide. After 2 h of natural drying, sections were fixed in methanol for 5 min followed by incubation with *anti*-RCTL antibody (1:100) in antibody dilution buffer without Triton X-100 overnight at 4 °C. The next-day steps are the same as the above-described paraffin sections. The DNA was stained by incubation with 4′,6-diamidino-2-phenylindole (DAPI, Beyotime, China). Results were visualized with a microscope (Zeiss Axioplan 2, Germany) equipped with a scan head (Bio-Rad MRC1024ES, USA).

2.7. Bacterial recognition and agglutination assay

Bacterial cells of *Arcobacter nitrofigilis* (ATCC33309) and *E. coli* (Beyotime, China) were cultured in their own optimizational medium. Cells were harvested by centrifugation at 6300 *g* for 5 min when OD_{600} reached 0.6 and then washed three times using TBS buffer (50 mM Tris-HCl, 100 mM NaCl, 10 mM $CaCl_2$, pH 7.5). In the microbial agglutination assay, bacteria were resuspended in TBS buffer to a final density of OD_{600} = 0.3 and incubated with rRCTL (100 μg/mL) at room temperature for 30 min. The GST protein was used as the control. To detect Ca^{2+} dependency, the same experiment was carried out in the buffer with 10 mM Ca^{2+} or with 10 mM EDTA. Agglutinating reactions were observed by microscopy (Zeiss LSM710 NLO, Germany). All the assays were performed in triplicate.

For statistics of agglutination experiments, different concentrations (100, 30 and 10 μg/mL) of rRCTL were added to the *E. coli* cultured in LB medium (containing 10 mM $CaCl_2$) during the mid-logarithmic phase and the agglutination of the bacteria was recorded by microscopy at different time points (30, 60, 90 and 120 min) at room temperature. The degree of agglutination is statistically analyzed by ImageJ [26]. The cell numbers were analyzed by OD_{600} measured by NANO Drop (Thermo Fisher Scientific, USA) after disintegration by adding D-mannose. Control groups were prepared by adding the same concentrations of the GST protein instead of rRCTL.

2.8. Carbohydrate binding specificity assay

The carbohydrate binding specificity was examined using the same method mentioned above in the microbial agglutination assay with some modification. Only *E. coli* was used in the experiment. The rRCTL using in the assay was incubated with five monosaccharides (D-glucose, D-galactose, D-fructose, D-mannose and *N*-acetyl-D-(+)-glucosamine) and two disaccharides (sucrose and maltose) at four concentrations (50, 100, 200 and 400 mM). The same buffer for dissolving the sugars was used as the positive control. The experiment was repeated three times.

2.9. TEM and SEM analysis

For TEM (transmission electron microscope) analysis, the sample was fixed with 2.5% glutaraldehyde in phosphate buffer (0.1 M, pH 7.0) overnight, washed three times in PBS for 15 min at each step, post fixed with 1% OsO_4 (in phosphate buffer) for 2 h and then washed three times in PBS for 15 min at each step. The specimen was first dehydrated by a graded series of ethanol (30%, 50%, 70%, 80%, 90%, 95% and 100%) for about 20 min at each time and finally transferred to absolute acetone for another 20 min. After incubation in a mixture of absolute acetone and spurr resin (equal volumes) for 1 h at room temperature, the specimen was transferred to a 1:3 (v/v) mixture of absolute acetone and spurr resin mixture for 3 h, and finally to spurr resin overnight. The sample was then placed in an eppendorf tube containing spurr resin and heated at 70 °C for more than 9 h. Finally, the pretreated specimen was sectioned with a microtome (Leica EM UC7, USA), stained by uranyl acetate and alkaline lead citrate each for 5–10 min, and observed with a transmission electron microscope (Gatan JEM-1230, Japan).

For SEM (scanning electron microscope) analysis, the pretreatment was performed under the same operations as TEM. After fixed with glutaraldehyde, whole setae of scaphognathites were washed and dehydrated in graded acetone series, and critical point dried with CO_2 using a critical point dryer (Hitachi HCP-2, Japan). Finally, the specimen was sputter coated with gold (Hitachi E-1010, Japan) and observed with a scanning electron microscope (Hitachi TM-1000, Japan).

2.10. Fluorescence in situ hybridization

We designed three oligonucleotide probes (Table 1) specific to 16S rRNA genes of the major ectosymbionts (γ-, ε- and δ-proteobacteria) in *R. exoculata*. All probes used were directly synthesized with fluorescently labeled on their 3′-ends (Sangon, China). FISH was performed according to a standard method [27] with modifications. Briefly, fixed scaphognathites dissected from *R. exoculata* was embedded and cut into five-micron slices as described above. Then the specimen was incubated at 46 °C in hybridization buffer (Roche, Switzerland) containing 35% formamide and respective probes. Hybridization was stopped by incubation in washing buffer (100 mM NaCl, 5 mM EDTA, 0.01% SDS, 20 mM Tris-HCl, pH 8.0) twice for 15 min at 48 °C. To stain DNA, the sections were covered in DAPI for 15 min. Finally, the slides were examined with a laser scanning confocal microscope (Zeiss LSM710 NLO, Germany).

2.11. Statistical analysis

All experiments were repeated three times and all data are given as the means ± S.D. for independent experiments. All statistical analyses were performed with SPSS 15.0 software. Comparative data were analyzed with Student's *t*-test. Significant and highly significant differences were defined as $P < 0.05$ and $P < 0.01$, respectively.

3. Results

3.1. Sequence analysis of RCTL

Based on analysis of a transcriptome from the *Rimicaris exoculata* scaphognathite (unpublished data), a full-length cDNA sequence was identified as C-type lectin (termed RCTL) by a BLAST retrieval in GenBank and sequence-validated by amplification of specific primers (Table 1). The RCTL cDNA is 1361 bp in length and contains an open reading frame (ORF) (nt 197–1142) that encodes a polypeptide of 314 amino acids with a calculated molecular mass of 35.1 kDa (Fig. 1A). It contained a predicted signal peptide (aa 1–18), an additional low-density lipoprotein receptor domain class A (LDLa, aa 20–60) and a conserved carbohydrate recognition domain (CRD, aa 152–305) that always exists in the CTL-family members. RCTL shows identities of 30.7–43.9% with other LDLa domain-containing CTLs from crustaceans (Fig. 1B). The calcium binding site and two couples of six cysteine residues forming disulfide bridges in LDLa and CRD domains are highly conserved. Typically, the key motif for sugar binding in crustacean CRDs is EPN or QPD which was specific for glucose/mannose or galactose binding, respectively. Phylogenetic analysis was performed based on amino acid sequences of C-type lectins from non-vent crustaceans. The unrooted tree (Fig. 1C) placed RCTL in all C-type lectins containing an LDLa domain at the *N*-terminus that divergent from those with one or two CRDs. However, as other crustacean LDLa domain-containing CTLs, a variant QAP was found in RCTL's CRD. Visualized by SwissModel, the CRD exhibits a common CLR fold, an overall loop structure with five N- and C- terminal β-sheets and two flanking α-helices (Fig. 1D).

3.2. Tissue expression pattern of RCTL

In order to understand the tissue expression pattern of RCTL, four tissues of *R. exoculata* were selected, including gills, muscle, hepatopancreas and scaphognathites (the main symbiotic organ). The transcription levels of RCTL in these tissues were determined by real-time PCR amplified with specific primers (Table 1). It revealed that the RCTL mRNA transcription level in scaphognathites was significantly higher than those in other tissues ($P < 0.01$; Fig. 2A). We further examined the protein level of RCTL in the same four tissues by Western blot with *anti*-RCTL antibody (HuaAn, China; Fig. S3). The result indicated that the RCTL was expressed predominantly in scaphognathites compared to the other tested tissues (Fig. 2B).

3.3. Characterization of symbionts and correlations with RCTL expression

Ectobiont diversity of setae on *R. exoculata* scaphognathites was studied by 16S rRNA pyrosequencing and prokaryotic transcriptome analysis (unpublished data). Two types of filamentous symbionts dominate (> 90% in richness) in *R. exoculata*: one 'thick' filament (2–3 μm) belonging to ε-proteobacterium and the other 'thin' filament (0.5–1 μm) belonging to γ-proteobacterium. Besides, another proteobacterial type belonging to δ-proteobacterium was spotted on the seta surface (Fig. 3A–B). FISH observations confirmed the correspondence between morphotypes and genotypes (Fig. 3C). Notably, the ε-proteobacterium were mainly distributed on one side of the setae, γ-proteobacterium surrounded the setae surface and δ-proteobacterium in short rods resided on the surface.

To study whether or not there are quantitative associations between the symbiotic bacteria and RCTL, immunofluorescence was performed on the setae of scaphognathites dissected from *R. exoculata* by *anti*-RCTL antibody. Large amounts of the RCTL protein were detected in the setae coating with bacteria filaments (Fig. 3D). Furthermore, we used real-time PCR to calculate correlations between the expression level of RCTL and number of each symbiont, by amplifying with RCTL- and each 16S RNA-specific primers, respectively (Table 1). By analyzing data from different *R. exoculata* individuals ($N = 3$), strong linear relationships were observed between RCTL and both ε- and γ-proteobacteria ($R^2 = 0.964$ and 0.971, respectively) but not δ-proteobacterium ($R^2 = 0.003$) (Fig. 3E).

3.4. rRCTL-directing agglutination of cultivable bacteria

Two reference cultivable bacteria of ε-proteobacterium (*Arcobacter nitrofigilis*) and γ-proteobacterium (*Escherichia coli*) were used in the bacterial recognition and attachment assays. After reaction for 1 h at room temperature, the recombinant RCTL (rRCTL; Fig. S2) was only able to recognize and agglutinate *E. coli* in a Ca^{2+}-dependent manner. No agglutination was observed when adding the GST protein or EDTA as control groups (Fig. 4A). To confirm this result and further verify the way through which rRCTL binds to the bacteria, we performed

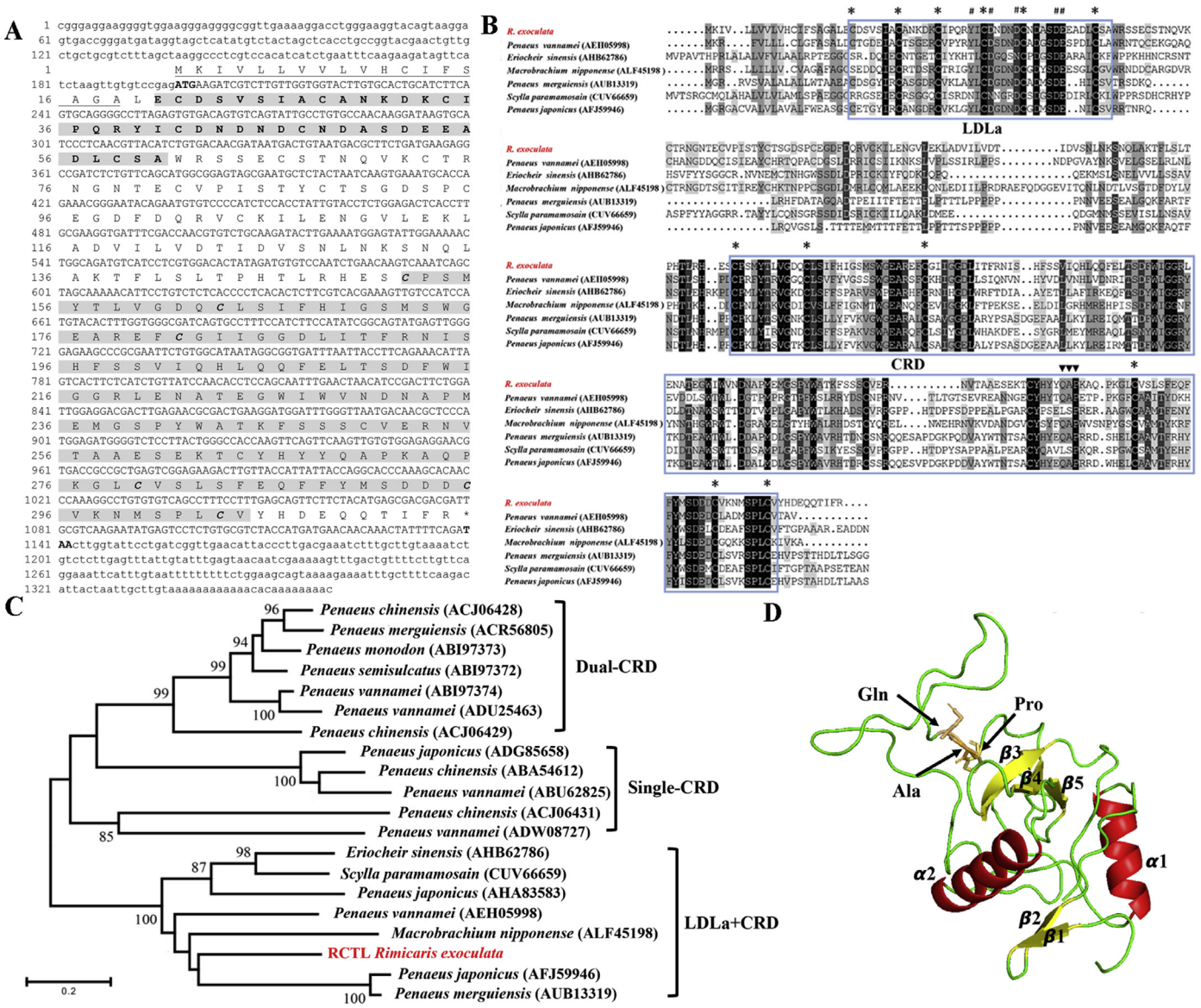

Fig. 1. Molecular analyses of RCTL. (A) The full-length RCTL cDNA of *R. exoculata.* Numbers in the left indicate the nucleotide (below) and amino acid (above) sequences. The signal peptide is underlined. The carbohydrate recognition domain (CRD) are gray shaded and conserved cysteine residues are depicted in bold font. The low-density lipoprotein receptor domain is gray shaded and in bold font. Start and stop codons are shown in bold font only. (B) ClustalW alignment of amino acid sequence of RCTL with those of other crustacean LDLa domain-containing C-type lectins. The LDLa and CRD domains are shown in boxed and six conserved cysteines therein are marked with asterisks. The QAP motif is indicated by arrowheads. Amino acids formed as a calcium binding site are marked with hashtags. GenBank accession numbers of each lectin are shown in figure. (C) Phylogenetic analysis of C-type lectins from crustaceans. GenBank accession numbers of each lectin are shown in the figure. Bootstrap values ≥ 75 are depicted beside nodes. The scale bar at the left-bottom represents the branch length corresponding to 0.2 difference per amino-acid residue. (D) A predicted three-dimensional model of the CRD of RCTL. Orange sticks depict the carbohydrate binding motif (QAP). Yellow, *β* sheets; red, *α* helices; green, random coils. (For interpretation of the references to colour in this figure legend, the reader is referred to the Web version of this article.)

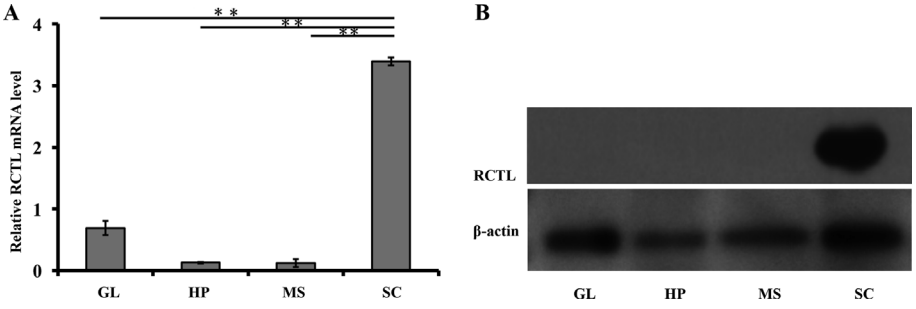

Fig. 2. Characterization of RCTL expression patterns. (A) RCTL mRNA levels in four tissues (GL: gills; SC: scaphognathites; MS: muscle; HP: hepatopancreas), revealed by real-time PCR. Vertical bars represent the mean ± S.D. ($N = 3$). The statistically significant differences indicated with ** represent $P < 0.01$. (B) Western blotting analysis of RCTL. Equal amounts of tissue proteins were hybridized with *anti*-RCTL antibody. An *anti-β*-actin antibody was used to detect the control protein *β*-actin.

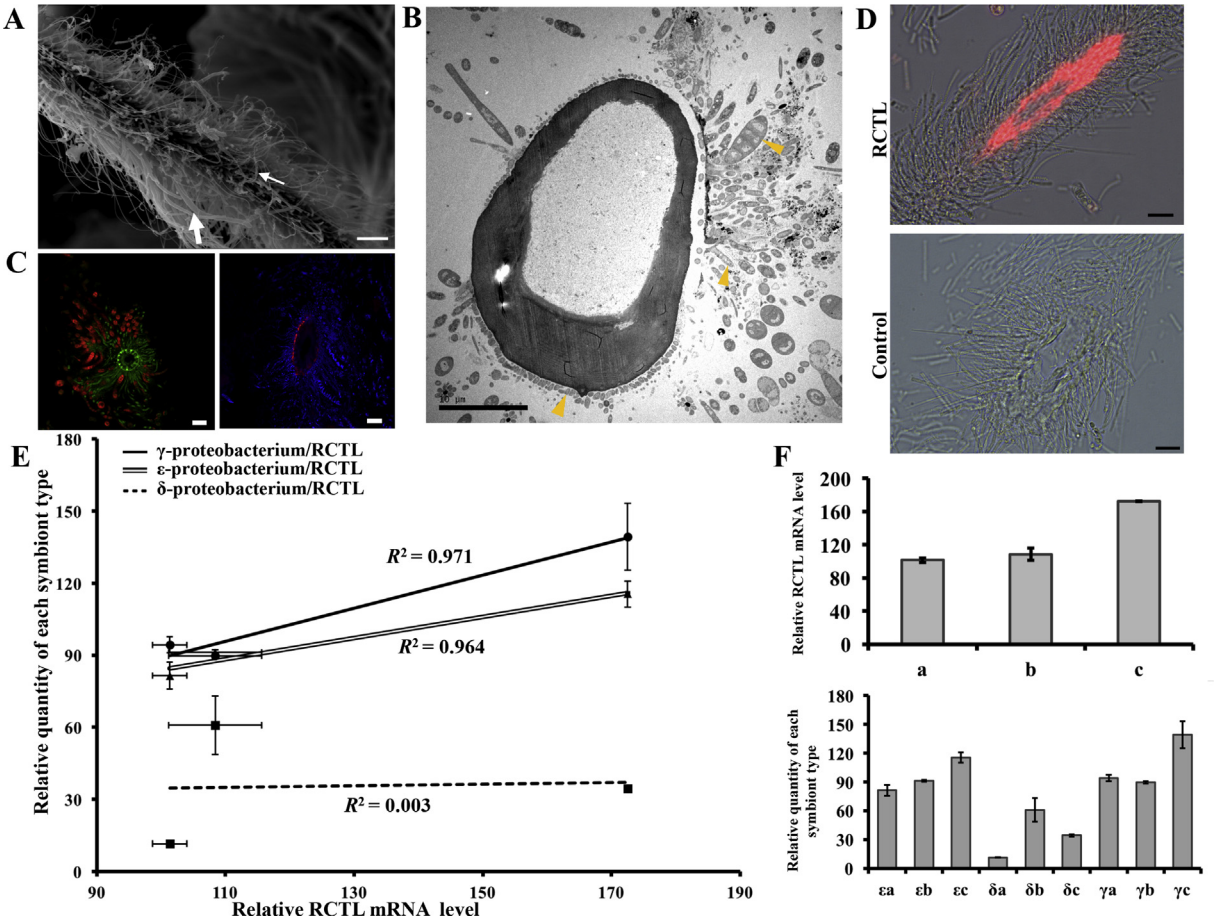

Fig. 3. Characterization of *R. exoculata* symbionts and relationship with RCTL expression. (A) A scanning electron microscopic image showing the filamentous symbionts on scaphognathite setae of *R. exoculata*. A 'thick' or 'thin' filament is indicated with a large or small arrow, respectively. Scale bar = 50 μm. (B) A transmission electron microscopic image showing general view of the transverse section of a scaphognathite seta and the associated bacteria. Arrowheads indicate several morphotypes of commensal bacteria. Scale bar = 10 μm. (C) Fluorescence *in situ* hybridization (FISH) of cross sections through scaphognathite setae of *R. exoculata*. ε- (red), γ- (green) or δ-proteobacterium (red) was hybridized by the EPSY105, GAM615 or DELT241 probe, respectively. DAPI staining is shown in blue. Scale bars = 20 μm. (D) Immunofluorescent analysis of RCTL. Cross-section of one scaphognathite seta was detected with *anti*-RCTL antibody. No signal was found in the control. Scale bars = 20 μm. (E) Linear regression analyses of quantities of symbiotic bacteria (ε, δ and γ-proteobacteria) and relative expression of RCTL. Linearity is defined as $R^2 > 0.9$. Vertical and horizontal bars represent the mean ± S.D. ($N = 3$). (F) Relative expression levels of RCTL from three shrimp individuals (a–c) by real-time PCR (above) and relative quantities of the three types of symbionts from the same three individuals (below). εa–εc, δa–δc and γa–γc: ε-, δ- and γ-proteobacteria from the three shrimps (a–c), respectively. (For interpretation of the references to colour in this figure legend, the reader is referred to the Web version of this article.)

immunofluorescence experiments with *anti*-RCTL antibody after rRCTL was added to *E. coli*. The result showed that the RCTL signal was co-located with the *E. coli* clumps (Fig. 4B). No binding was observed when using the GST protein as a control.

To verify whether or not the agglutination of the microbes is carbohydrate-dependent, inhibition of agglutination was performed by using various monosaccharides and disaccharides showing in Table 2. Four concentrations (50, 100, 200 and 400 mM) were assayed for each sugar. No adding carbohydrate was used as the positive control. Compared to the control, 200 mM of D-glucose, D-mannose and maltose could inhibit *E. coli* agglutination induced by RCTL, while the inhibition caused by sucrose occurred at the concentration of 400 mM. D-galactose, D-fructose and *N*-acetyl-D-(+)-glucosamine alone showed no inhibitory effect on the agglutinating activity realized by rRCTL even when each concentration reached 400 mM (Table 2). From the results, we speculated that rRCTL preferred to recognizing glucose and mannose, which might be concerned with the specificity between RTCL and the symbiont MAMP(s).

3.5. Characterization of RCTL-bacteria interaction

To further investigate the working pattern of the RCTL-bacteria interaction, three different concentrations (10, 30 and 100 μg/mL, final concentrations) of rRCTL were added to *E. coli*, followed by recording with microscopy at different time points (30, 60, 90 and 120 min). In each rRCTL-added group, the bacteria were significantly clumped by the protein compared to the control of GST (Fig. 5A). According to the statistical analysis, the agglutination degrees (measured by $\log_2$ (particle areas)) in the 100 μg/mL rRCTL groups exhibitted stronger than those in lower rRCTL concentrates at all time points. Meanwhile, with the rRCTL concentrations increasing or time going by, the agglutination degrees elevated as well (Fig. 5B). Moreover, in all rRCTL-treated groups *E. coli* exhibited normal growth curves as the control, which meant that the growth of the recruited *E. coli* had never been affected by agglutination (Fig. 5C).

4. Discussion

Deep-sea hydrothermal vents are generally characterized by great spatial and temporal instability. Due to everlasting darkness, life here

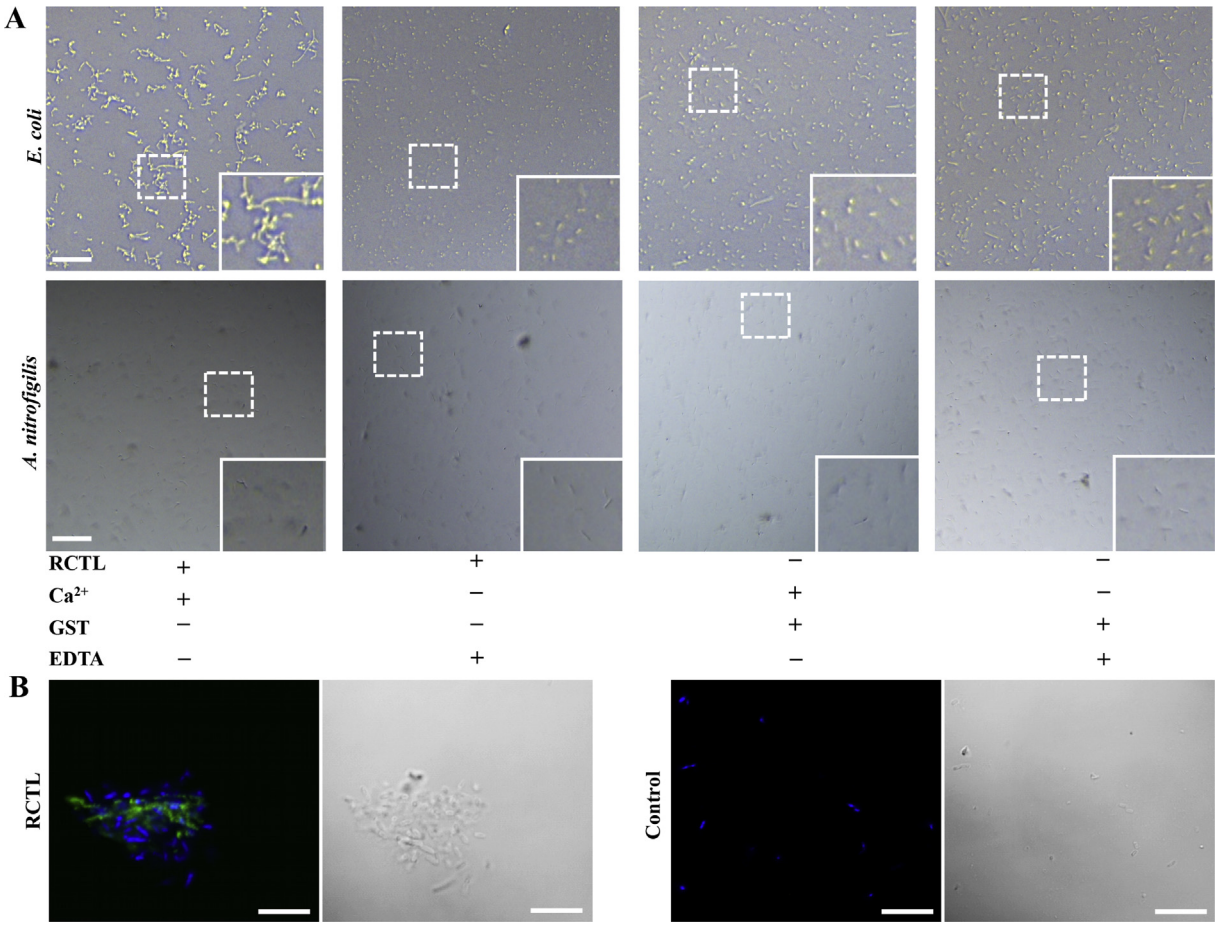

Fig. 4. Bacterial recognition and attachment assays. (A) Bacterial (*Arcobacter nitrofigilis* and *Escherichia coli*) recognition and agglutination by rRCTL in a Ca^{2+}-dependent manner. The GST protein was used as the negative control. (B) Binding of *E. coli* by rRCTL visualized on a confocal microscope. Bacteria were stained with DAPI (blue) and rRCTL were detected by *anti*-RCTL antibody (green). Scale bars = 10 μm. (For interpretation of the references to colour in this figure legend, the reader is referred to the Web version of this article.)

Table 2
Sugar inhibition of microbial agglutinating activity of RCTL.

Inhibitor	Minimum concentration for inhibition (mM)
D-glucose	200
D-galactose	NA
D-fructose	NA
D-mannose	200
N-acetyl-D-(+)-glucosamine	NA
sucrose	400
maltose	200

NA: no inhibition of agglutination at the indicated concentration (400 mM).

can't extract energy to drive anabolism from the sun like photoautotrophs on the earth surface. However, amazing biomasses of large organisms thrive under this seemly extremity, such as tubeworms, gigantic clams, crabs, shrimps and so on [28–30]. Most of them have evolved different forms of symbiotic relationships with microbes [31,32], such as endosymbioses in tubeworms and clams, or ectosymbioses in crabs and shrimps. The symbiotic bacteria, usually originating from free-living chemoautotrophs, can utilize chemical reductants in venting fluid for producing energy to support biosynthesis of important metabolites like carbohydrates.

As a dominant fauna at MAR hydrothermal vents, the bresiliid shrimp *Rimicaris exoculata* has a large number of ectosymbiotic bacteria in its gill chamber especially on the specialized organ of scaphognathites [33]. At the present study, microscopies and FISH revealed that three major types of proteobacteria attached outside of the setae covering the whole scaphognathites: one sulfide-oxidizing γ-proteobacterium absolutely dominating the symbionts, another sulfide/hydrogen-oxidizing ε-proteobacterium and a probable sulfur-reducing δ-proteobacterium. The close-related bacteria have been found in the ambient seawater or deposit environment [34,35], indicating their local origins and recruit reservoirs. Like most hydrothermal-vent animals that horizontally regain symbioses between generations, *R. exoculata* renews its ectosymbiotic bacteria even after each molt of exoskeleton where the symbionts attach. Although the relative richnesses of different symbionts showed variable at different stages of molt [10], the taxonomic compositions of *R. exoculata* symbioses kept stable wherever the shrimp was collected from along the vent sites of MAR. The most important problem the shrimp has to deal with in the process of symbiosis recovery is how to select and enrich the fixed group of symbiotic microbes from relative low richnesses of environmental candidates.

Previous studies have revealed that recognition between the host pattern recognition receptors (PRRs) and microbe-associated molecular patterns (MAMPs) is a vital initial step where the host and microbe interact. In invertebrates, pathogenesis or symbiosis share the common recognition process that induces different resultant cascades – rejective destruction or mutualistic coexistence, respectively [13]. Naturally our purpose would aim to find highly expressed PRR molecules in the symbiotic organ of *R. exoculata*, the scaphognathite. By analyzing a transcriptome of scaphognathites (unpublished data), one high-expressed molecule belonging to the lectin superfamily of PRRs came to our sight. The putative peptide has a LDLa domain, a conserved carbohydrate recognition domain (CRD) and six conserved cysteine

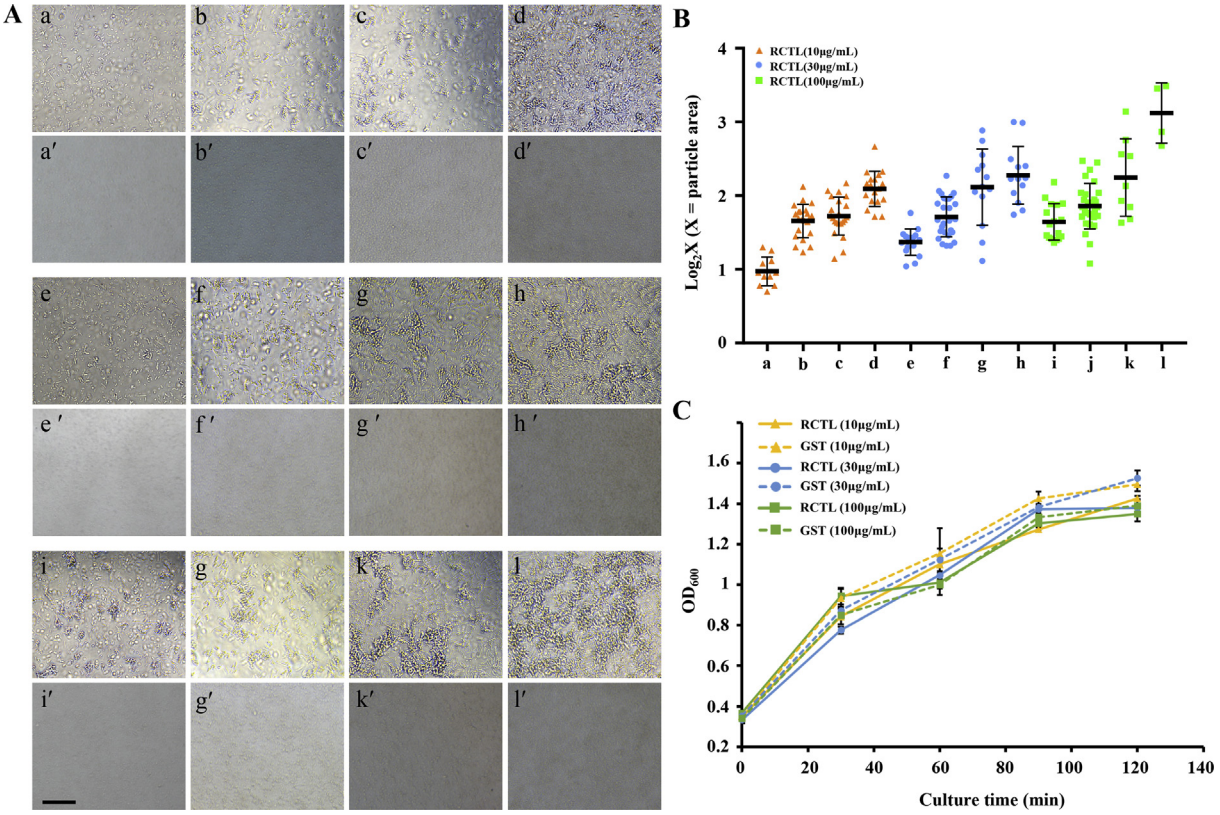

Fig. 5. Association of RCTL with bacterial cells. (A) *E. coli* agglutination induced by rRCTL in the presence of 10 mM $CaCl_2$ at four different time points (30, 60, 90 and 120 min, by column). The GST-treatment was used as the control. a–d, a'–d': 10 μg/mL; e–h, e'–h': 30 μg/mL; i–l, i'–l': 100 μg/mL. Scale bar = 10 μm. (B) Statistical analysis of recruited *E. coli* at each rRCTL concentration/time point consistent with (A). (C) Effects of rRCTL on bacterial growth, displayed by growth curves of *E. coli* in (A) with or without rRCTL.

residues forming disulfide bridges. Phylogenetic analysis also showed that RCTL was grouped with lectins with LDLa + CRD domains and separated from those with one or two CRDs. Lectins with multiple domains found in invertebrates usually have a broader spectrum of microbial recognition and a stronger binding affinity with carbohydrates on the surface of pathogens. In the case of the additional LDLa domain, although it has not been clearly studied so far, some researchers did indicate that it could enhance the ability of lectins to recognize and bind bacteria. For example, the *Eriocheir sinensis* C-type lectin EsCTLDcp with a LDLa domain showed an enhanced activity of binding to *Bacillus thuringiensis* [36]. Similar evidence was found in the shrimp *Fenneropenaeus merguiensis* [37]. We speculate that the LDLa domain in RCTL might be concerned with its specific recognition and agglutination of bacterial symbionts. By a prediction of three-dimensional structure, a mixture of α/β units of featured CTL-type CRD was identified. All the results indicate that the molecule is a member of C-type lectins (CTLs), which we termed RCTL. Although symbiosis-related CTLs have been identified in nematode (Mermaids) [20], coral (millectin) [13], and clam (codakine) [21], this is the first time a similar molecule is found in crustaceans.

It was observed that RCTL predominantly expressed in scaphognathites, at both mRNA and protein levels. The RCTL mRNA was seemly transcribed more ubiquitously while its protein almost specifically appears in scaphognathites. One explanation is, as an original immune-related molecule, different doses of the RCTL mRNA might exist everywhere as a synthetic potential in case of emergency, while the exclusive enrichment of the RCTL protein in scaphognathites might reflect its main function of agglutinating symbionts therein. The results of immunofluorescence also detected strong signals on setae of scaphognathites, the actual location where the symbionts inhabit. Unlike most shrimp CTLs that are highly expressed in hepatopancreas suggesting their immune functionalities against pathogens [11], the absolute abundance of RCTL in scaphognathites but not hepatopancreas also indicates its potential role in the symbiosis of *R. exoculata*. More and more researchers have reached a consensus that the expression of these innate-immune genes reflects its symbiotic lifestyle and status [38,39], and meanwhile, the quantity and type of symbionts can also affect the host's transcriptomic regulation [40]. In *R. exoculata* the biggest challenge to stable symbiotic maintanance is the cyclic process of molting that always eliminates the bacteria by removing the old exoskeleton and will have to recover symbioses by recolonization. Despite lacking of serial samples of molting stages due to technical difficulties in sampling, we still tried investigating the relationships between RCTL expression and quantities of different symbionts, by analyzing several shrimp individuals. For the three major ectosymbionts, clear linear relationships were found between RCTL expression and the numbers of γ- and ε-proteobacteria but not δ-proteobacterium. Although it is seemly not the only participant, RCTL might still play an important role in the selection of the *R. exoculata* symbioses.

There are two difficulties in clarifying the relationship between RCTL and symbiotic bacteria. First, despite high expression in scaphognathites, natural RCTL from several shrimp individuals was still not enough for a comprehensive elucidation. We therefore prokaryotically overexpressed RCTL and used the purified recombinant protein (rRCTL) for bacterial binding experiments. Second, all *R. exoculata* ectosymbionts are uncultivable to date, which meant that we had to resort to their cultivable substitutes. Here, we chose two reference bacteria: a γ-proteobacterium (*Escherichia coli*) and ε-proteobacterium (*Arcobacter nitrofigilis*). The result of binding assay showed that rRCTL could only recognize and agglutinate *E. coli* but not the other, in a Ca^{2+}-dependent manner. Immunofluorescence localized rRCTL in the middle of the agglutinated bacterial cells. Moreover, when we added

fluorescent rhodamine-labeled rRCTL onto a small fraction of scaphognathites, a morphotype of 'thin' filamentous bacteria was clearly visualized (Fig. S1), which seemed γ-proteobacteria discriminated by the size and morphology suggested by a previous study [4,41]. In summary, RCTL might play a vital role in recognition and enrichment of the γ-proteobacterium of *R. exoculata*.

Based on the interaction between rRCTL and the γ-proteobacterium of *E. coli*, we made further investigations. First, the specificities of rRCTL to different saccharide units implied characteristics of MAMPs constituting basis of symbiotic selectivity. To recognize and non-covalently bind specific glycoproteins and glycoconjugates on the microbial surface and agglutinate bacterial cells through carbohydrate recognition domains (CRDs) is the most important function of CTLs [42]. Mutation analyses revealed that carbohydrate-binding specificity could be changed by conversion of the motif sequence [43,44]. Generally in a CRD, a EPN motif shows specific to glucose/mannose, and a QPD motif shows specific to galactose. However, there are variations of these two motifs in some CTLs [11]. In our research, rRCTL could recognize monosaccharides of mannose and glucose, as well as disaccharides with one glucose residue (sucrose and maltose). Although more carbonhydrate specificities should be verified, RCTL did select compatible partners by recognizing a limited group of glycans. Second, the effect of rRCTL on bacterial growth is one of important features to discriminate between symbiotic or pathogenic microbes, and further maintain the stability of symbioses. One key aspect of maintaining a stable symbiosis is that the symbionts do not overgrow the host and the host does not eliminate the symbionts. In *R. exoculata*, the results of agglutination experiments illustrated that the bacterial recruiting level of RCTL showed a clear dose-dependent and time-cumulative pattern. Besides, the addition of rRCTL had no significant effect on bacterial growth throughout the process. All evidence shows that RCTL might play important roles in achieving the selectivity of beneficial microbes as well as maintaining the stability of symbioses.

5. Conclusion

In conclusion, we identified a C-type lectin (RCTL) from the deep-sea hydrothermal-vent shrimp *R. exoculata.* The high expression levels in scaphognathites where ectosymbionts inhabit, as well as clear linear correlationships with quantities of two major symbiotic bacteria, implied its important role in symbiosis of the shrimp. rRCTL was able to selectively recognize and agglutinate the cultivable γ-proteobacterium of *E. coli* in a Ca^{2+}-dependent manner. This function was presumable proposed by recognizing and non-covalently binding specific carbohydrate ligands on the microbial surface. Unlike conventional crustacean C-type lectins, rRCTL didn't affect the normal growth of the bacteria that had been recruited, but showed a dose- and time-cumulative pattern on the process of agglutination. These features are similar to those of the natural recolonization and proliferation of the symbionts after each molt cycle of the host. As one of the most important steps in the establishment of highly specific mutualistic associations, this is the first key molecule analyzed in a deep-sea vent shrimp and will shed light on understanding their adaptive evolution in such a special environment.

Conflicts of interest

The authors declare that there is no conflict of interest.

Acknowledgement

We thank Dr. Zongze Shao and Yingbao Gai [Third Institute of Oceanography, Ministry of Natural Resources, Xiamen, Fujian 361005, PR China] for providing the invaluable samples of *Rimicaris exoculata*. This work was supported by the 973 Program of China [Grant Numbers 2015CB755903]; the National Key R&D Program of China [Grant Number 2018YFD0900603]; the National Natural Science Foundation of China [Grant Numbers 41376133 and 41406175]; and the Natural Science Foundation of Zhejiang Province [Grant Number LY18C040002].

Appendix A. Supplementary data

Supplementary data to this article can be found online at https://doi.org/10.1016/j.fsi.2019.05.057.

References

[1] D. Desbruyères, A. Almeida, M. Biscoito, et al., A review of the distribution of hydrothermal vent communities along the northern Mid-Atlantic Ridge: dispersal vs. environmental controls, Hydrobiologia 440 (1–3) (2000) 201–216 https://doi.org/10.1023/A:1004175211848.
[2] A.B. Williams, P.A. Rona, Two new caridean shrimps (Bresiliidae) from a hydrothermal field on the Mid-Atlantic Ridge, J. Crustac Biol. 6 (3) (1986) 446–462 https://doi.org/10.1163/193724086x00299.
[3] H. Michael, J.M. Petersen, D. Nicole, et al., Pathways of carbon and energy metabolism of the epibiotic community associated with the deep-sea hydrothermal vent shrimp *Rimicaris exoculata*, PLoS One 6 (1) (2011) e16018 https://doi.org/10.1371/journal.pone.0016018.
[4] M. Zbinden, N.L. Bris, F. Gaill, et al., Distribution of bacteria and associated minerals in the gill chamber of the vent shrimp *Rimicaris exoculata* and related biogeochemical processes, Mar. Ecol.: Prog. 284 (1) (2004) 237–251 https://doi.org/10.3354/meps284237.
[5] C.L.V. Dover, B. Fry, J.F. Grassle, et al., Feeding biology of the shrimp *Rimicaris exoculata*, at hydrothermal vents on the Mid-Atlantic Ridge, Mar. Biol. 98 (2) (1988) 209–216 https://doi.org/10.1007/BF00391196.
[6] J.M. Petersen, A. Ramette, C. Lott, et al., Dual symbiosis of the vent shrimp *Rimicaris exoculata* with filamentous gamma- and epsilonproteobacteria at four Mid-Atlantic Ridge hydrothermal vent fields, Environ. Microbiol. 12 (8) (2010) 2204–2218 https://doi.org/10.1111/j.1462-2920.2009.02129.x.
[7] M. Zbinden, B. Shillito, N.L. Bris, et al., New insigths on the metabolic diversity among the epibiotic microbial communitiy of the hydrothermal shrimp *Rimicaris exoculata*, J. Exp. Mar. Biol. Ecol. 359 (2) (2008) 131–140 https://doi.org/10.1016/j.jembe.2008.03.009.
[8] J. Ponsard, M.A. Cambonbonavita, M. Zbinden, et al., Inorganic carbon fixation by chemosynthetic ectosymbionts and nutritional transfers to the hydrothermal vent host-shrimp *Rimicaris exoculata*, ISME J. 7 (1) (2013) 96–109 https://doi.org/10.1038/ismej.2012.87.
[9] M. Bright, S. Bulgheresi, A complex journey: transmission of microbial symbionts, Nat. Rev. Microbiol. 8 (3) (2010) 218–230 https://doi.org/10.1038/nrmicro2262.
[10] M. Guri, L. Durand, V.C. Gauchard, et al., Acquisition of epibiotic bacteria along the life cycle of the hydrothermal shrimp *Rimicaris exoculata*, ISME J. 6 (3) (2012) 597–609 https://doi.org/10.1038/ismej.2011.133.
[11] X.W. Wang, J.X. Wang, Diversity and multiple functions of lectins in shrimp immunity, Dev. Comp. Immunol. 39 (1–2) (2013) 27–38 https://doi.org/10.1016/j.dci.2012.04.009.
[12] L. Cerenius, P. Jiravanichpaisal, H.P. Liu, et al., Crustacean Immunity, Springer US, 2010, https://doi.org/10.1007/978-1-4419-8059-5-13.
[13] E.C.E. Kvennefors, W. Leggat, O. Hoegh-Guldberg, et al., An ancient and variable mannose-binding lectin from the coral *Acropora millepora* binds both pathogens and symbionts, Dev. Comp. Immunol. 32 (12) (2008) 1582–1592 https://doi.org/10.1016/j.dci.2008.05.010.
[14] S.R. Coats, A.B. Berezow, T.T. To, et al., The lipid A phosphate position determines differential host toll-like receptor 4 responses to phylogenetically related symbiotic and pathogenic bacteria, Infect. Immun. 79 (1) (2011) 203–210 https://doi.org/10.1128/IAI.00937-10.
[15] T.A. Koropatnick, Microbial factor-mediated development in a host-bacterial mutualism, Science 306 (5699) (2004) 1186–1188 https://doi.org/10.1126/science.1102218.
[16] U. Hentschel, H. Felbeck, Nitrate respiration in the hydrothermal vent tubeworm *riftia pachyptila*, Nature 366 (6453) (1993) 338–340 https://doi.org/10.1038/366338a0.
[17] B.B. Bohlool, E. L. Schmidt Lectins, A possible basis for specificity in the rhizobium–legume root nodule symbiosis, Science 185 (4147) (1974) 269–271 https://doi.org/10.1126/science.185.4147.269.
[18] W.E. Müller, R.K. Zahn, B. Kurelec, et al., Lectin, a possible basis for symbiosis between bacteria and sponges, J. Bacteriol. 145 (1) (1981) 548–558.
[19] S.S. Manoharan, V.P.W. Miao, S. Andrésson, LEC-2, a highly variable lectin in the lichenPeltigera membranacea, Symbiosis 58 (1–3) (2012) 91–98 https://doi.org/10.1007/s13199-012-0206-y.
[20] S. Bulgheresi, I. Schabussova, T. Chen, et al., A new C-type lectin similar to the human immunoreceptor DC-SIGN mediates symbiont acquisition by a marine nematode, Appl. Environ. Microbiol. 72 (4) (2006) 2950–2956 https://doi.org/10.1128/AEM.72.4.2950-2956.2006.
[21] J.P. Gourdine, A. Markiv, J. Smith-Ravin, The three-dimensional structure of codakine and related marine C-type lectins, Fish Shellfish Immunol. 23 (4) (2007) 831–839 https://doi.org/10.1016/j.fsi.2007.03.009.
[22] K.K. Ng, S. Parksnyder, W.I. Weis, Ca^{2+} dependent structural changes in C-type mannose-binding proteins, Biochemistry 37 (51) (1998) 17965–17976 https://doi.

org/10.1021/bi981972a.
[23] S. Kumar, G. Stecher, K. Tamura, MEGA7: molecular evolutionary genetics analysis version 7.0 for bigger datasets, Mol. Biol. Evol. 33 (2016) 1870–1874 https://doi.org/10.1093/molbev/msw054.
[24] G. Janson, C. Zhang, M.G. Prado, et al., PyMod 2.0: improvements in protein sequence-structure analysis and homology modeling within PyMOL, Bioinformatics 33 (3) (2016) 444–446 https://doi.org/10.1093/bioinformatics/btw638.
[25] B. Bubner, I.T. Baldwin, Use of real-time PCR for determining copy number and zygosity in transgenic plants, Plant Cell Rep. 23 (5) (2004) 263–271 https://doi.org/10.1007/s00299-004-0859-y.
[26] T.J. Collins, ImageJ for microscopy, Biotechniques 43 (1 Suppl) (2007) 25–30 https://doi.org/10.2144/000112517.
[27] A. Moter, U.B. Göbel, Fluorescence in situ hybridization (FISH) for direct visualization of microorganisms, J. Microbiol. Methods 41 (2) (2000) 85–112 https://doi.org/10.1016/S0167-7012(00)00152-4.
[28] C. Tan, C.D. Cino, K. Ding, W.E. Seyfried, High temperature hydrothermal vent fluids in Yellowstone lake: observations and insights from *in-situ* pH and redox measurements, J. Volcanol. Geotherm. Res. 343 (2017) 263–270 https://doi.org/10.1016/j.jvolgeores.2017.07.017.
[29] E. Ramirezllodra, T.M. Shank, C.R. German, Biodiversity and biogeography of hydrothermal vent species: thirty years of discovery and investigations, Oceanogr. Soc. 20 (2007) 30–41 https://doi.org/10.5670/oceanog.2007.78.
[30] G. Beedessee, H. Watanabe, T. Ogura, et al., High connectivity of animal populations in deep-sea hydrothermal vent fields in the Central Indian Ridge relevant to its geological setting, PLoS One 8 (2013) e81570 https://doi.org/10.1371/journal.pone.0081570.
[31] J. Klose, M.F. Polz, M. Wagner, et al., Endosymbionts escape dead hydrothermal vent tubeworms to enrich the free-living population, Proc. Natl. Acad. Sci. U.S.A. 112 (36) (2015) 11300–11305 https://doi.org/10.1073/pnas.1501160112.
[32] T. Ikuta, Y. Takaki, Y. Nagai, et al., Heterogeneous composition of key metabolic gene clusters in a vent mussel symbiont population, ISME J. 10 (4) (2015) 990–1001 https://doi.org/10.1038/ismej.2015.176.
[33] J.M. Petersen, A. Ramette, C. Lott, et al., Dual symbiosis of the vent shrimp *Rimicaris exoculata* with filamentous gamma- and epsilonproteobacteria at four Mid-Atlantic Ridge hydrothermal vent fields, Environ. Microbiol. 12 (8) (2010) 2204–2218 https://doi.org/10.1111/j.1462-2920.2009.02129.x.
[34] G.E. Flores, J.H. Campbell, J.D. Kirshtein, et al., Microbial community structure of hydrothermal deposits from geochemically different vent fields along the Mid-Atlantic Ridge, Environ. Microbiol. 13 (8) (2011) 2158–2171 https://doi.org/10.1111/j.1462-2920.2011.02463.x.
[35] T. Cerqueira, D. Pinho, C. Egas, et al., Microbial diversity in deep-sea sediments from the Menez Gwen hydrothermal vent system of the Mid-Atlantic Ridge, Mar. Genom. 24 (2015) 343–355 https://doi.org/10.1016/j.margen.2015.09.001.
[36] Y. Huang, L. An, K.M. Hui, et al., An LDLa domain-containing C-type lectin is involved in the innate immunity of *Eriocheir sinensis*, Dev. Comp. Immunol. 42 (2) (2013) 333–344 https://doi.org/10.1016/j.dci.2013.10.004.
[37] P. Kwankaew, R. Praparatana, P. Runsaeng, et al., An alternative function of C-type lectin comprising low-density lipoprotein receptor domain from, *Fenneropenaeus merguiensis*, to act as a binding receptor for viral protein and vitellogenin, Fish Shellfish Immunol. 74 (2018) 295–308 https://doi.org/10.1016/j.fsi.2017.12.044.
[38] J. Wippler, M. Kleiner, C. Lott, et al., Transcriptomic and proteomic insights into innate immunity and adaptations to a symbiotic lifestyle in the gutless marine worm *Olavius algarvensis*, BMC Genomics 17 (1) (2016) 942 https://doi.org/10.1186/s12864-016-3293-y.
[39] L. Steindler, S. Schuster, M. Ilan, et al., Differential gene expression in a marine sponge in relation to its symbiotic state, Mar. Biotechnol. 9 (5) (2007) 543–549 https://doi.org/10.1007/s10126-007-9024-2.
[40] I. Boutet, R. Ripp, O. Lecompte, et al., Conjugating effects of symbionts and environmental factors on gene expression in deep-sea hydrothermal vent mussels, BMC Genomics 12 (1) (2011) 530 https://doi.org/10.1186/1471-2164-12-530.
[41] S. Fujiyoshi, H. Tateno, T. Watsuji, et al., Effects of hemagglutination activity in the serum of a deep-sea vent endemic crab, *Shinkaia crosnieri*, on non-symbiotic and symbiotic bacteria, Microb. Environ. 30 (3) (2015) 228–234 https://doi.org/10.1264/jsme2.ME15066.
[42] H.L. And, N. Sharon, Lectins: carbohydrate-specific proteins that mediate cellular recognition, Chem. Rev. 98 (2) (1998) 637–674 https://doi.org/10.1021/cr940413g.
[43] M.J. Mandel, M.S. Wollenberg, E.V. Stabb, et al., A single regulatory gene is sufficient to alter bacterial host range, Nature 458 (7235) (2009) 215–218 https://doi.org/10.1038/nature07660.
[44] X. Wei, L. Wang, W. Sun, et al., C-type lectin B (SpCTL-B) regulates the expression of antimicrobial peptides and promotes phagocytosis in mud crab *Scylla paramamosain*, Dev. Comp. Immunol. 84 (2018) 213–229 https://doi.org/10.1016/j.dci.2018.02.016.